Macroscopic criteria for the deformation and fracture of iron based alloys

Dina V. Orlova, Alexey G. Lunev, Lidiya V. Danilova, Lev B. Zuev
Institute of Strength Physics and Materials Science SB RAS, 2/4 Akademicheskii Ave., 634055 Tomsk, Russia
dvo@ispms.tsc.ru

ABSTRACT. In the article the deformation of different steels is analyzed using the autowave theory of plasticity. The article considers the possible use of an autowave model to formulate criteria for the structural strength of materials and elastic-plastic transition. The time and place of future fracture for steel samples are shown can be predicted before visible necking takes place by using the kinetic dependencies of localized plasticity domains at the pre-fracture stage. The results show that during elastic-plastic transition in low-carbon steel, there is the break of the curve for the ultrasound velocity versus deformation, which can serve as an acoustic criterion of irreversible deformation for the pressure treatment of metals, the operation and non-destructive testing of products and structures.

KEYWORDS. Steels, Ductile Fracture; Ultrasound Velocity; Digital Speckle Photography.

Citation: Orlova, D.V., Lunev, A.G., Danilova, L.V., Zuev, L.B., Macroscopic criteria for the deformation and fracture of iron based alloys, Frattura ed Integrità Strutturale, 42 (2017) 293-302.

Received: 04.07.2017
Accepted: 15.08.2017
Published: 01.10.2017

INTRODUCTION

At present, the critical parts and structures of many hazardous production facilities operate under mechanical loads which initiate the occurrence and accumulation of damages leading to the fracture of equipment. These damages can be timely identified and eliminated if appropriate technical means and methods are available. In this connection, special attention is paid to the problem concerning the objective and reliable estimation of the mechanical condition and the prediction of the resource for critical elements and structures in the long operation.

Since the localized development of a plastic flow has a significant effect on the strength and plastic characteristics of structural steel products, it is of importance to describe the kinetics of a plastic flow and the transition from deformation to ductile fracture.

The progressive development of the dislocation theory using high-resolution techniques, mainly electron microscopy, allowed a number of efficient models to be developed for the strain and impurity hardening of metals, as well as for the micromechanics of fracture [1-9]. Nevertheless, the kinetics of a plastic flow was not insufficiently described. It is difficult to add the time factor to the equations of plasticity. For example, the Taylor-Orowan equation obtained for this purpose

is valid only for certain chaotic distributions of dislocations, when their density is considered to be independent of coordinates [10]. That is, beginning with the Griffith's [9] hypothesis about the existence of places for the initiation of cracks, deformation criteria consider local characteristics for the development of cracks and the structural parameters of materials. Also, the microscopic approach was mainly used to consider the physics of material fracture. Therefore, the complete description of a plastic flow only on the basis of micromechanisms is impossible.

Thus, inefficient dislocation models in the physics of strength and plasticity were replaced with the complex concept of a multilevel approach. A multiscale approach to the problems of plastic deformation and fracture was developed due to the works of domestic and foreign researchers [11-19] and currently is used by the scientific community.

Thus, at present a deformable material is considered to be a nonlinear medium, an appropriate description of which is impossible without the approach based on the concepts for the mechanics of nonlinear media, synergetics and nonlinear acoustics. So, using the synergetic approach describing the self-organization of highly nonequilibrium systems, the authors of this article and coworkers found a new type of wave processes in a solid. Any plastically deformed object is known to be under nonequilibrium conditions [20]. In order to describe strain, it is proposed to consider a deformed macroobject to be an active medium that includes two factors: activator and inhibitor. Moreover, localized shear processes are considered to be an activator, and the redistribution of local stresses connected with these processes is considered to be an inhibitor. This was the basis for the autowave model for the evolution of localized macrodeformation [21-24]. In contrast to ordinary waves described by hyperbolic equations, autowaves are the solutions of parabolic equations, an important feature of which is the presence of a time derivative, which determines their applicability for the description of reversible processes [25-26]. Autowaves are formed only in the media with energy dissipation and when there are external nonperiodic effects. From this point of view, the strain of any object represents the evolution of autowaves during different type deformation. The change in the type of autowaves is determined by the law of strain hardening, that is, it depends on the stages of the strain flow curve (rule of correspondence). Thus, the movement of a solitary deformation front is observed within the yield plateau (the work hardening coefficient $\theta = 0$) along the sample, the so-called autowave excitation or switching. At the linear stage ($\theta = const$) there is the coordinated movement of localization zones (phase autowaves). The stationary structure of zones (stable dissipative systems) corresponds to the stages of parabolic hardening $\left(\sigma \sim \varepsilon^{1/2}, \theta \sim \varepsilon^{-1/2}\right)$. A stationary high-amplitude zone (domain) of localized plasticity is formed in the sample at the place of future fracture at the final stage of the deformation process (pre-fracture stage), and the movement of other localized plasticity domains is nonuniform but self-coordinated. This article is devoted to deep studying the macrolocalization of plastic deformation at this stage. In addition, the authors of this article believe that a complex approach based on a combined analysis of the plastic flow localization during the deformation process and supplemented by the simultaneous measurement of small changes in the velocity of ultrasound propagation should be applied to the problem concerning the reliable estimation of the mechanical condition and the prediction of the resource for structures in the long operation. This will allow us to determine the exact location of the places with damages and find a connection with a localized plastic flow.

Recently, an acoustic analysis of materials under loading has been developed in the field of plastic deformation in theoretical and experimental studies by Kobayashi [27, 28], Maurel [29], Zuev [30]. At present, individual groups of researchers only start developing such an approach, mainly by using idealized simple model media. For real materials used in technological production and materials with a complex structure, such an integrated approach has not been developed yet.

Thus, the aim of the work is to study the stage of pre-fracture for iron based alloys and analyze the possible use of an autowave model to formulate criteria for the structural strength of materials and elastic-plastic transition. The last fact will allow an important technological problem to be solved and the behavior of structural materials to be controlled before the initiation of irreversible plastic deformation. Since the inhomogeneity or localization of deformation is manifested not only in the accumulation of defects during the operation of constructions, but also in many technological processes connected with pressure treatment, drawing, etc., the estimation of material plasticity is an urgent problem for these processes.

MATERIALS AND EXPERIMENTAL PROCEDURES

Steel of different composition was chosen as test materials. Heat-resistant stainless steel (AISI 420), cryogenic structural steel (321N), carbon steel (G10080), and electrical steel (alloy of iron and silicon) were used. These iron based alloys are widely used not only in industry, but in experimental studying the physics of plasticity and strength.

For example, silicon iron chosen by Amelinckx and Hull [31, 32] is a traditional material for investigating the mechanisms of plastic flow and fracture. The elemental composition of the test steels is given in Tab. 1. The samples were obtained using sheet semi-fabricated products subjected to pressing and recrystallization annealing. In the mechanical tests, flat samples were in the form of a double blade 2×10×50 mm in size.

Steels	C	Cr	Ni	Si	Mn	Cu
AISI 420	0.35-0.45	12-14	≤0.6	≤0.8	≤0.8	≤0.3
321H	≤0.12	17-19	9-11	≤0.8	≤2.0	≤0.3
G10080	0.05-0.11	0.1	≤0.25	0.05-0.17	0.35-0.65	≤0.25
Fe-Si alloy	-	-	-	2.8-3.8	-	-

Table 1: Chemical compositions of experimental steels, in wt.%.

The samples were subjected to uniaxial loading at room temperature and a constant velocity of $6.67 \cdot 10^{-5}$ s^{-1} by using the one universal testing machine head (Walter + Bai, Switzerland), the second testing machine head was fixed.
The initial load curves of all materials $\sigma(\varepsilon)$ were recalculated into true stresses s and strain e, the relationship between which was described by the Ludwik's equation $s(e) = s_0 + Ke^n$ [33], where K is the work hardening coefficient, and n is the hardening exponent. To determine the stages of the plastic flow, the dependence $s(e)$ was taken in the logarithmic form. The sections corresponding to the stages of the plastic flow are easily separated when the curve $s(e)$ is transformed into the coordinates $\ln(s - s_0) - \ln e$, and represented by the straight lines for $K = const$ and $n = const$. The hardening exponent $n = 0$ corresponds to the yield plateau, $n = 1$ corresponds to the linear stage, and $n = 0.5$ corresponds to the parabolic stage of strain hardening. The continuous pre-fracture stage, for $n < 0.5$, was observed for all materials (Tab. 2).
The stress-strain state of objects in the real time mode, visualization of deformation and fracture localization zones were investigated by speckle interferometry, described in detail in [34, 35]. The method allows the patterns of plastic deformation localization to be recorded by fixing the displacement fields of points for a deformed sample.
The use of a two-exposure speckle photograph and the analysis of the speckle structure for the images of deformed objects are very promising for investigating the features of plastic deformation at the macroscale level. This technique is successfully used in solving similar problems [36, 37].
The method is valid in the field of vision about 100 mm in size and has a measuring accuracy of 1 μm for displacement vectors. A series of sequential specklegrams reflecting the displacement field of the sample points for an increase in the total strain of 0.2% was recorded within the yield plateau for the steel (G10080) and at the pre-fracture stage for all the materials studied. Using the data on the displacement fields and numerical coordinate differentiation, all components for the tensor of the plastic material distortion can be determined for the plane case: local narrowing, local elongation, shift and rotation. Then, the data on the displacement fields for the points of a deformed sample are transformed into the distributions of local elongations ε_{xx}, where the localized plasticity domains are clearly separated.
The propagation velocity of ultrasonic Rayleigh waves was used as an acoustic informative parameter at a frequency of 5 MHz. Using this type of waves allows the propagation of ultrasound velocity in the sample to be kept constant during experiments. To measure the propagation velocity of Rayleigh waves, a transmit-receive sensor was used, which contained transmitting and receiving piezoelectric transducers installed in the same enclosure and based on piezoceramics (CTS-19) with a resonance frequency of 5 MHz. Piezoelectric transducers are installed at an angle of 56° to the normal to the incidence plane of an acoustic wave, which provides the formation of a surface acoustic wave (Rayleigh wave) in iron based alloys. The distance between the transducers (the length of the acoustic path in the test object) without considering the length of the sensor waveguide was 32 mm. The propagation velocity of Rayleigh waves was determined by the ratio between the path length of a wave in the sample and the delay time for the signal of the receiving transducer relative to the transmitting one. The delay time was measured using an oscillogram recorded with a digital oscilloscope at a sampling frequency of 2 GHz. The measurement accuracy was 10^4 – 10^5.

EXPERIMENTAL RESULTS AND DISCUSSIONS

Stress-strain curves and propagation of elastic surface Rayleigh waves

Fig. 1 and 2 show the stress-strain curves of the test materials. It is seen that these curves are parabolic and can be used to determine the stages in accordance with the law of strain hardening. The fracture is ductile, and there is well visible necking in the samples. The mechanical characteristics and length of the section with the n < 0.5 are given in Tab. 2. The exception is the σ-ε curve for carbon steel G10080 (Fig.2). The feature of this curve is the presence of a tooth and a yield plateau typical for carbon steels [38]. The length of the yield plateau is 0.013 < e < 0.047 (3.4%). The strain within the yield plateau is known to be in the form of the Luders band [39].

Steels	σ_y, MPa	$\sigma_{0.2}$, MPa	δ,%	Pre-fracture stage, $n < 0.5$
AISI 420	1183	420	6.0	$0.033 < e < 0.05$ (1.7 %)
321H	178	512	55	$0.45 < e < 0.55$ (10 %)
G10080	310	210	40	$0.25 < e < 0.35$ (10 %)
Fe-Si alloy	590	320	25	$0.064 < e < 0.22$ (15.6 %)

Table 2: Mechanical properties of the samples and the length of the pre-fracture stage.

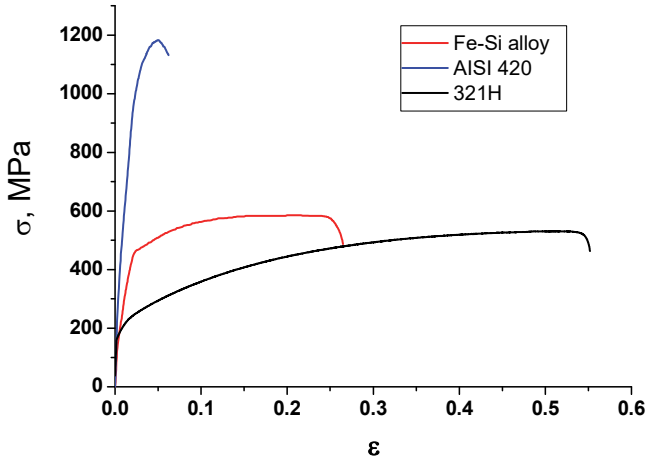

Figure 1: Stress-strain curves of the test materials.

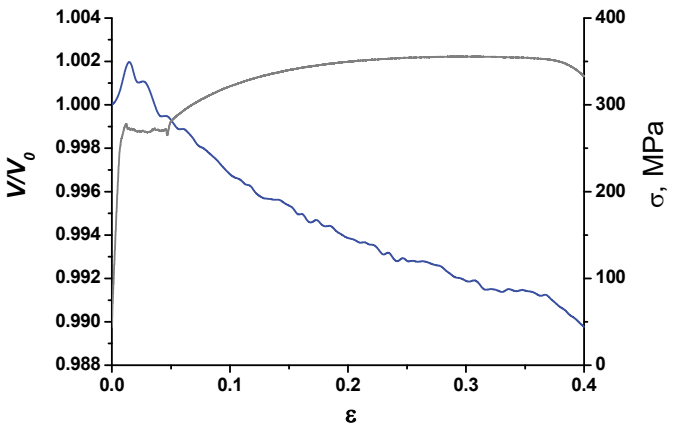

Figure 2: Stress and relative sound velocity versus the strain of steel (G10080).

The measurement of acoustic characteristics within the yield plateau is of great interest. The position of the Luders bands and the change in the propagation velocity of ultrasonic Rayleigh waves in steel (G10080) within the yield plateau were recorded simultaneously with the deformation of the sample. In Fig. 3, the σ-ε loading diagram is plotted by a light gray line, and the yield plateau is accompanied by the formation of the Luders band front near the lower testing machine head. The position of the Luders band fronts is plotted in the form of black circles (black lines). The deformation is accompanied by the propagation of the two Luders band fronts at a velocity of 0.052 mm/s and 0.038 mm/s. The region of the sample in which the change in the velocity of ultrasonic waves is recorded is indicated by two horizontal dashed lines. Red markers indicate the entry of the Luders band fronts in the ultrasonic velocity measurement area. It should be noted that the formation of the Luders band out of the acoustic measurement area is accompanied by the increase in the velocity of ultrasonic waves. When the fronts move to the area of acoustic measurements, a maximum is formed on the V(ε) curve and the ultrasound velocity starts decreasing, since the front moves inside the acoustic measurement area.

During plastic deformation, two types of stresses has an effect on the propagation velocity of ultrasonic waves: macrostresses caused by an external applied load [40] and microstresses caused by the evolution of the dislocation structure [27-29, 41]. The formation of the Luders band leads to the fact that the stresses in the sample are localized in the Luders band, and the stresses in the remaining volume of the sample are decreased. This leads to an increase in the ultrasound velocity. The propagation of the localized deformation front is accompanied by the increase in the dislocation

density and, as a consequence, by the decrease in the ultrasound velocity, which is observed when the Luders fronts move in the acoustic measurement area.

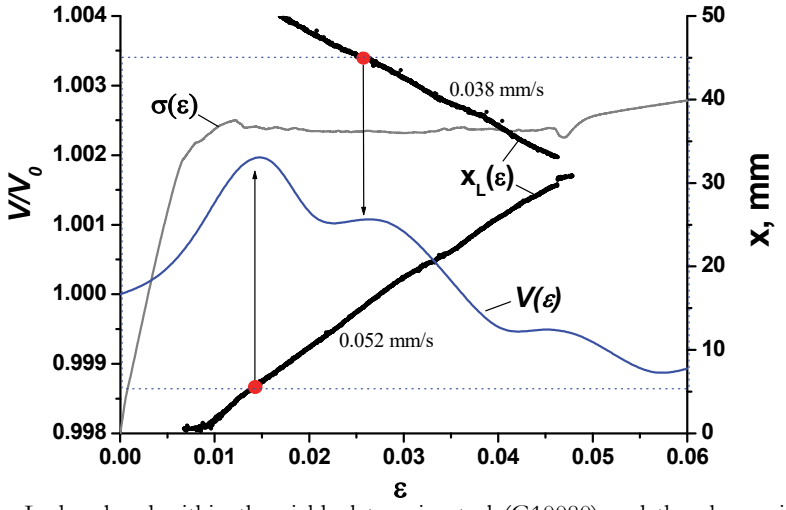

Figure 3: Propagation of the Luders band within the yield plateau in steel (G10080) and the change in the velocity of ultrasonic Rayleigh waves.

Development of localized plastic deformation at the pre-fracture stage n <0.5

Fig. 4 shows localized deformation versus time for all test alloys. The position of the localized deformation domains is indicated by colored symbols. The time sequence of the localized plasticity domains allows the number of macrostrain zones and their rate to be determined using the slope of curves (displacement coordinate - time (*X-t*)). Thus, 4 movable deformation zones and one fixed maximum of deformation localization are formed in steel (G10080) at the pre-fracture stage (Fig. 4a). Such a stationary zone of localized plasticity has the highest amplitude. Fig. 5 shows the distribution of local strain ε_{xx} along the sample at the beginning and at the end of the pre-fracture stage.

At the pre-fracture stage, when the index of strain hardening is $n < ½$, the localized plasticity domains start moving along the tension axis, approaching the high-amplitude zones mentioned above, which were stationary before fracture.

During the movement of localized plasticity domains, the values of their velocities become mutually consistent. The farther the localization zone is located from a stationary zone, the higher its velocity is (Tab. 3). This leads to the fact that all zones reach simultaneously the stationary zone of localization, and the graphs for the positions of the movable zones versus time create the bundle of straight lines with the center coordinates of X^* and t^*. Often, the extrapolation of the dependence $X(t)$ is required for large time to determine X^* and t^*. According to the experimental data of all the materials studied, the location of the sample fracture also coincides with the position of the stationary localization zone. Thus, the question concerning the stationary zone position and, consequently, the pole of the zone movement at the pre-fracture stage acquires a special meaning.

For the quantitative description of the kinetics for the zones at the pre-fracture stage, it is reasonable to combine the origin of coordinates with the stationary localization zone. In this case, the coordinate of an arbitrary zone ξ_i is determined by

$$\xi_i = X_i - X_0, \tag{1}$$

where X_0 and X_i are the coordinates of the stationary localization zone and arbitrary zone in the laboratory coordinate system, the origin of which coincides with the fixed testing machine head. In the reference system chosen in this way, the zone movement graphs form a sheaf of straight lines with a single pole, when the velocities of the zones are linearly dependent on their coordinates ξ_i, that is the following relation is met:

$$V_i(\xi) = \alpha\xi_i + \alpha_0 \tag{2}$$

where α and α_0 are the empirical constants.

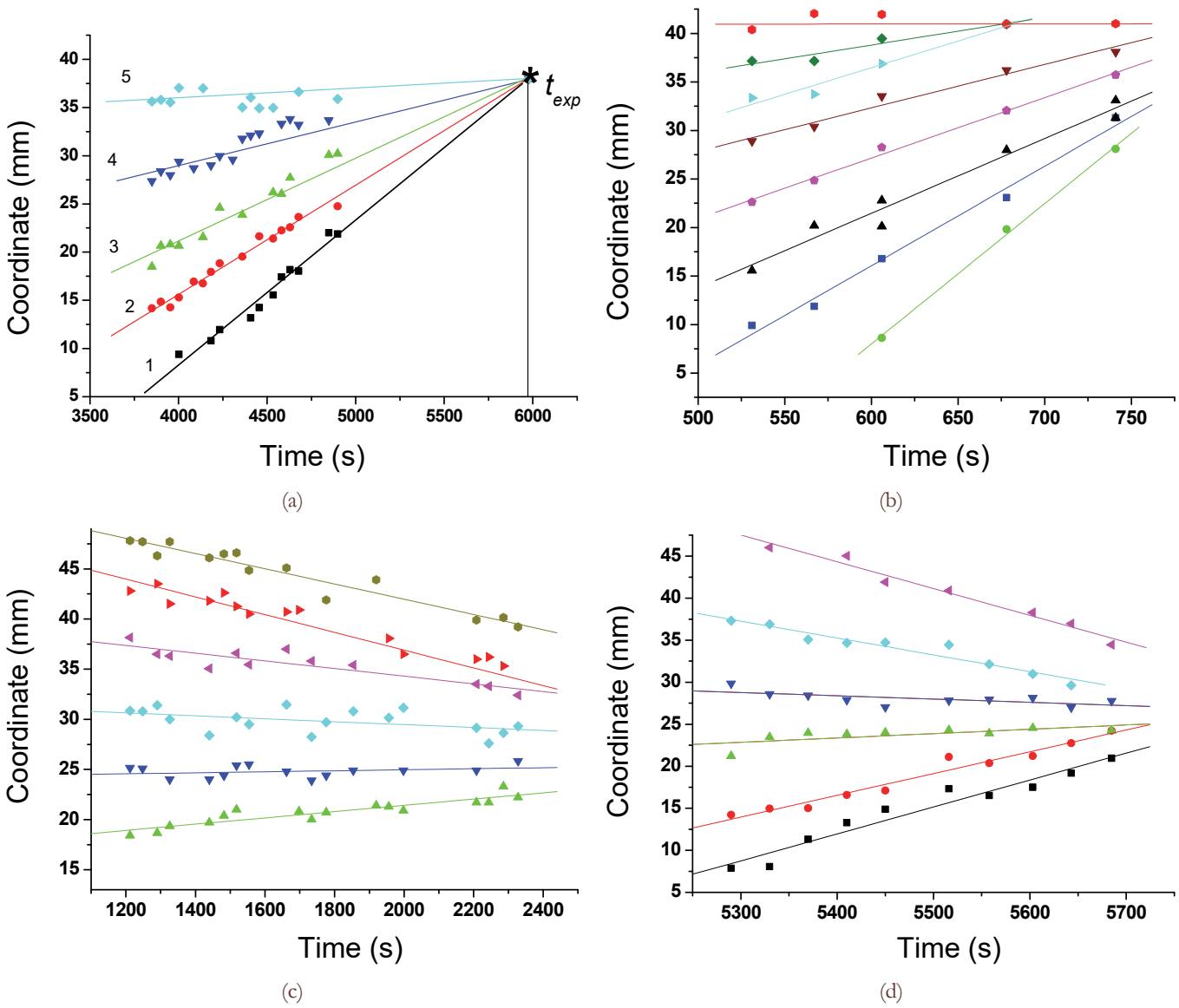

Figure 4: Movement of localized plasticity domains at the stage n <0.5: a - for steel (G10080); b - for steel (AISI 420); c - for silicon iron; d - for steel (321H).

For the obtained dependences $X(t)$, the pole is not always identified. However, the position of poles can always be shown if the linear dependence (2) is met. Let us consider the calculation for steel (G10080). It is seen that the pole is reached at the moment of time 5978 s, and the self-consistent movement of the zones begins at t_0 = 4003 s (Fig. 4a). The coordinate of the stationary localization zone for steel (G10080) is $X_{S.Z.}$ = 35.85 mm from the stationary testing machine head. According to the data in Tab. 3, the velocity of deformation zones was obtained versus the initial coordinates $V_{av}(\xi)$ (Fig. 6). The constants a and α_0 are determined experimentally by the method of least squares, in this case α_0 = 0.0018 and α = 4.98·10^{-4}. Fig. 6 also shows that the dependence $V(\xi)$ obtained for all test alloys is linear.

Domain, №	1	2	3	4	5
ξ, mm	26.47	20.58	15.19	6.48	0
V_i×10^6, m·s^{-1}	0.15	0.11	0.1	0.07	0.0031

Table 3: Velocities of the deformation zones at the pre-fracture stage for steel (G10080).

The analysis of the α and α_0 coefficients showed that $\alpha_0 = 1/t$, where t is the time for the movement of zones at the pre-fracture stage, and the ratio $\xi^* = \alpha/\alpha_0$ is the deviation of the pole from a stationary zone. Then, in the laboratory reference system the location of the pole and the time required for reaching the pole by the localization zones are given by:

$$X^* = X_0 + \xi^* = X_0 + \alpha \ / \alpha_0 \tag{3a}$$

$$t^* = t_0 + 1/\alpha \tag{3b}$$

where t_0 is the time when a pre-fracture stage is formed. The position of the pole and the time required for reaching the pole, calculated according to (3a) and (3b) for steel (G10080), were X^* = 39.5 mm and t^* = 6011 s. In fact, the sample was fractured in 5978 s after deformation at a distance of 38 mm from the fixed testing machine head. It can be seen that the space-time coordinates of the pole and the experimental values of location and fracture time are in satisfactory agreement. Tab. 4 shows the calculated values of location and fracture time for other materials. The calculated values obtained were compared with the real coordinates and fracture time of different materials. It is seen that the difference does not exceed 11%.

Thus, the kinetic characteristics obtained for the autowaves of localized plasticity at the pre-fracture stage, which can be found experimentally, allow the space-time coordinates of the object fracture to be predicted long before the occurrence of external fracture signs. This can be used as a macroscopic criterion for the plasticity of structural steels and alloys.

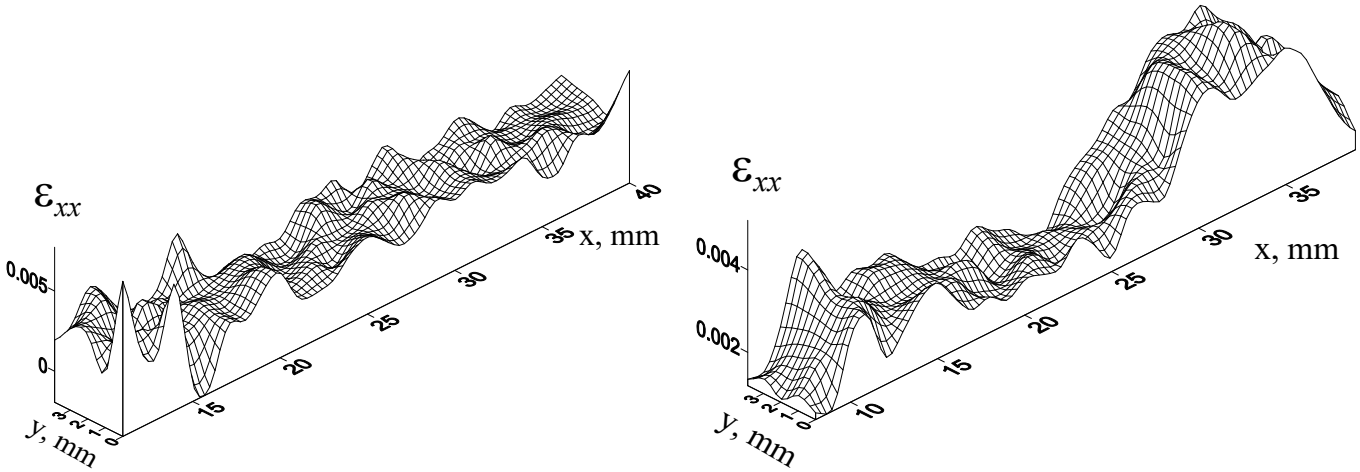

(a) (b)

Figure 5: Three-dimensional image of ε_{xx} at the beginning (a) and end (b) of the pre-fracture stage for steel (G10080).

Fracture time			Material	Fracture coordinate		
t^*_{exp}, c	t^*_{calc}, c	t^*_{exp}/t^*_{calc}		X^*_{exp}, mm	X^*_{calc}, mm	X^*_{exp}/X^*_{calc}
5978	6011	0.99	G10080	38	39.5	0.96
6620	5895	1.11	321H	25	27	0.93
4014	3679	1.09	Fe+3%Si	35	35.5	0.99
930	871	1.07	AISI 420	43	42	1.02

Table 4: Comparison of the experimental and calculated coordinates and the fracture time of the samples.

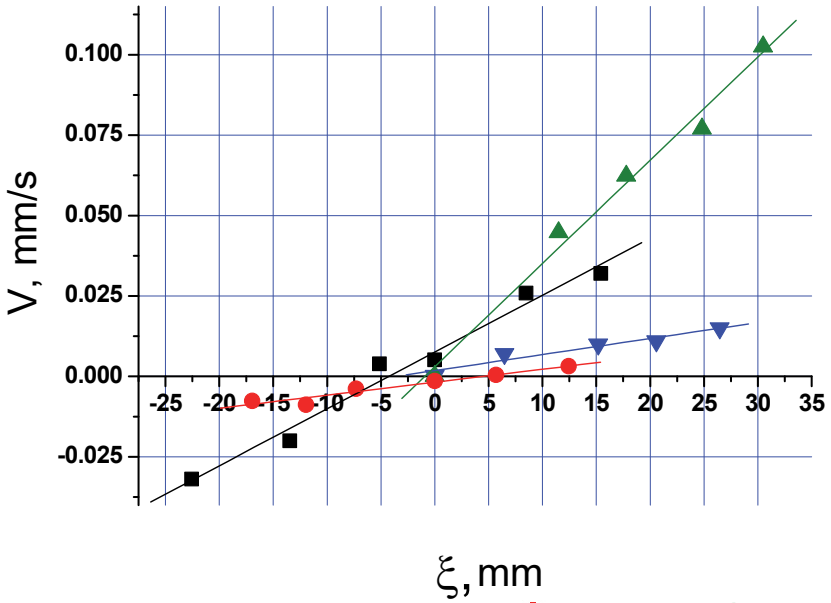

Figure 6: Dependencies of $V_{an}(\xi)$: for 321H (■); for G10080 (●); for AISI 420 (▲); for silicon iron (▼).

Conclusions

The deformation of metals and alloys is locally developed at all stages of a plastic flow, including elastic-plastic transition. During transition, dislocations actively move and spread in localization zones, and the density of dislocations is increased. This leads to a change in the characteristics for the propagation of acoustic waves. Thus, during the transition to the region of a plastic flow, there is the break of the curve for the velocity of ultrasonic Rayleigh waves versus the magnitude of deformation, and the increase is replaced with a drop. The break of the curve can serve as an acoustic criterion of irreversible deformation for the pressure treatment of metals, the operation and non-destructive testing of products and structures.

For large deformation, at the pre-fracture stage of iron based alloys, the deformation process is gradually stopped in the entire volume of the material, except the part of the material that directly adjoins the place of necking and a ductile crack. In terms of self-organization, there is the autowave collapse of localized plastic deformation [21]. The kinetic characteristics of the autowave collapse at the pre-fracture stage, which can be found experimentally, allow the space-time coordinates of the object fracture to be predicted long before the occurrence of external signs.

The work conducted contributes to the creation of a database on the mechanical and acoustic characteristics of alloys and steels both for elastic-plastic transition and large plastic deformations. This is necessary for the development of algorithms for predicting the resource of plasticity in the operation and manufacturing of parts and structures.

Acknowledgments

The work was supported by the Russian Foundation for Basic Research (project No. 16-19-10025).

References

[1] Cottrell, A.H., Bilby, B.A., Dislocation theory of yielding and strain ageing in iron, Proc. Phys. Soc. A, 62 (1949) 1-40.
[2] Kuhlmann-Wilsdorf, D., Dynamic effects in the mesh length theory of workhardening, Acta Metall., 37 (1989) 3217-3223.

[3] Johnston, W.G., Gilman, J.J., Dislocation velocities, dislocation densities, and plastic flow in lithium fluoride crystals, J. Appl. Phys., 30 (1959) 129 – 134.
[4] Kubin, L.P., Estrin, Y., Strain nonuniformities and plastic instabilities, Rev. Phys .Appl., 23 (1988) 573 – 583.
[5] Burgers, J.M., Geometrical considerations concerning the structural irregularities to be assumed in a crystal, Proc. Phys. Soc., 52 (1940) 23-33.
[6] Read, W.T., Shockley, W., Dislocation models of crystal grain boundaries, Phys. Rev., 78 (1950) 275 – 289.
[7] Estrin, Y., Toth, L.S., Molinari, A., Brechet, Y., A dislocation-based model for all hardening stages in large strain deformation, Acta Mater., 46 (1998) 5509-5522.
[8] Armstrong, R.W., Dislocation viscoplasticity aspects of material fracturing, Eng. Fract. Mech., 77 (2010) 1348-1359.
[9] Griffith, A.A., The phenomena of rupture and flow in solids, Philos. Trans. R. Soc., 221 (1921) 163–198.
[10] Orowan, E., Dislocations in Metals, AIME, New York, (1954).
[11] Panin, V.E., Egorushkin, V.E., Panin ,A.V., The plastic shear channeling effect and the nonlinear waves of localized plastic deformation and fracture, Phys. Mesomech., 13 (2010) 215-232.
[12] Panin ,V.E., Egorushkin, V.E., Deformable solid as a nonlinear hierarchically organized system, Phys. Mesomech., 14 (2011) 207-223.
[13] Ning, J., Aifantis, E.C., On the description of anisotropic plastic flow by the scale invariance approach, Int. J. Plasticity, 11 (1995) 183-193.
[14] Zaiser, M., Glazov, M., Lalli, L.A., Richmond, O., On the relations between strain and strain-rate softening phenomena in some metallic materials: a computational study, Comp. Mater. Sci., 15 (1999) 35-49.
[15] Zaiser, M., Avlonitis, M., Aifantis, E., Stochastic and deterministic aspects of strain localization during cyclic plastic deformation. Acta Mater., 46 (1998) 4143-4151.
[16] Chrysochoos, A., Louche, H., An infrared image processing to analyse the calorific effects accompanying strain localisation, Int. J. Eng. Sci., 38 (2000) 1759-1788.
[17] Inal, K., Wu, P.D., Neale, K.W., Instability and localized deformation in polycrystalline solids under plane-strain tension, Int. J. Solid. Struct. 39 (2002) 983-1002.
[18] Benallal, A., Berstad, T., Børvik, T., Clausen, A.H., Hopperstad, O.S. Dynamic strain aging and related instabilities: experimental, theoretical and numerical aspects, Eur. J. Mech, A-Solid, 25 (2006) 397–424.
[19] Sarmah, R., Ananthakrishna ,G., Influence of system size on spatiotemporal dynamics of a model for plastic instability: Projecting low-dimensional and extensive chaos, Phys. Rev. E, 87 (2013) 052907.
[20] Haken, H., Information and Self-Organization, Springer, Berlin, (1988).
[21] Zuev, L.B., On the waves of plastic flow localization in pure metals and alloys, Ann. Phys., 16 (2007) 286–310.
[22] Zuev, L.B., Barannikova, S.A., Experimental study of plastic flow macro-scale localization process: Pattern, propagation rate, dispersion, Int. J. Mech. Sci., 88 (2014) 1-7.
[23] Danilov, V.I., Orlova, D.V., Zuev, L.B. On the kinetics of localized plasticity domains emergent at the pre-failure stage of deformation process, Mater. Design, 32 (2011) 1554 – 1558.
[24] Zuev, L.B. Regularities of the localized plastic flow viewed as consequences of elastoplastic invariant of strain, Metallofiz.Noveishie Tekhnol., 38 (2016) 1335-1349.
[25] Evers, L.P., Brekelmans, W.A.M., Geers, M.G.D., Scale dependent crystal plasticity framework with dislocation density and grain boundary effect, Int. J. Solid Struct., 41 (2004) 5209-5230.
[26] Billingsley, J.P., The possible influence of the de Broglie momentum-wavelength relation on plastic strain 'autowave' phenomena in 'active materials', Int. J. Solid. Struct., 38 (2001) 4221-4234.
[27] Kobayashi, M., Ultrasound nondestructive evaluation of microstructural changes under plastic deformation, Int. J. Plasticity, 19 (2003) 511-522.
[28] Kobayashi, M., Analysis of deformation localization based on the proposed theory of ultrasonic wave velocity propagation in plastically deformed solids, Int. J. Plasticity, 26 (2010) 107-125.
[29] Maurel, A., Pagneux, V., Barra, F., Lund, F., Ultrasound as a probe of plasticity? The interaction of elastic waves with dislocations, Int. J. Bifur. Chaos, 19 (2009) 2765-2781.
[30] Barannikova, S., Lunev, A., Li, Yu., Zuev, L., Use of Acoustic Parameter Measurements for Evaluating the Reliability Criteria of Machine Parts and Metalwork, Key Eng. Mater., 743 (2017) 486-489.
[31] Amelinckx, S., The direct observation of dislocations, Academic Press., New York, (1964).
[32] Hull, D., Effect of grain size and temperature of slip, twining and fracture in 3% silicon iron, Acta Met., 9 (1961) 191-204.
[33] Honeycombe, R.W.K., The plastic deformation of metals, Edward Arnold Ltd., New York, (1968).
[34] Zuev, L.B., Danilov, V.I., A self-excited wave model of plastic deformation in solids, Philos. Mag., 79 (1999) 43-57.

[35] Jones, R., Wykes, C., Holographic and Speckle Interferometry, Cambridge Univ. Press., Cambridge, (1983).
[36] Hudson, R.R., Setopoulos, D.D. ,Speckle interferometric method for the determination of time-dependent displacement and strain. Strain., 11 (1975) 126-132.
[37] Aebischer, H.A., Waldner, S.. Strain distribution made visible with image-shearing speckle pattern interferometry, Opt. Laser. Eng., 26 (1997) 407-420.
[38] Shioya, T., Shiroiri, J., Elastic–plastic analysis of the yield process in mind steel, J. Mech. Phys. Solid, 24 (1974) 187–204.
[39] Mazière, M., Luisb, C., Maraisa, A., Foresta, S., Gaspérini, M., Experimental and numerical analysis of the Lüders phenomenon in simple shear, Int. J. of Solid and Struct., 106–107 (2017) 305–314.
[40] Riichi, M., Kazuhiro, M., Development of a non-contact stress measurement system during tensile testing using the electromagnetic transducer for a Lamb wave, NDT & E Int., 39 (2006) 299-303.
[41] Granato, A.V., Lucke, K., Theory of mechanical damping due to dislocations, J. Appl. Phys., 27 (1956) 583-593.